PCCP

ROYAL SOCIETY OF CHEMISTRY

PAPER

View Article Online
View Journal | View Issue

Cite this: *Phys. Chem. Chem. Phys.*, 2024, **26**, 11436

Mechanochemical hydroquinone regeneration promotes gold salt reduction in sub-stoichiometric conditions of the reducing agent†

Ismael P. L. Xavier, [a] Laura L. Lemos, [a] Eduardo C. de Melo, [a] Eduardo T. Campos, [a] Breno L. de Souza, [a] Leandro A. Faustino, [a] Douglas Galante [b] and Paulo F. M. de Oliveira *[a]

Bottom-up mechanochemical synthesis (BUMS) has been demonstrated to be an efficient approach for the preparation of metal nanoparticles (NPs), protected by surface agents or anchored on solid supports. However, there are limitations, such as precise size and morphological control, due to a lack of knowledge about the mechanically induced processes of NP formation under milling. In this article, we further investigate the BUMS of AuNPs. Using SiO_2 as a solid support, we studied the effect of typical reducing agents, namely $NaBH_4$, L-ascorbic acid, and hydroquinone (HQ), on the conversion of a Au^{III} source. XANES showed that HQ is the strongest reducing agent under our experimental conditions, leading to the quantitative conversion of gold salt in a few minutes. Interestingly, even when HQ was used in sub-stoichiometric amounts, Au^{III} could be reduced to ratios higher than 85% after two minutes of milling. Investigations into the byproducts by ^1H NMR and GC-FID/MS enabled the identification HQ regeneration and the formation of its derivatives. We mainly focused on benzoquinone (BQ), which is the product of the oxidation of HQ as it reduces the gold salt. We could demonstrate that HQ is regenerated from BQ exclusively under milling and acidic conditions. The regenerated HQ and other HQ-chlorinated molecules could then reduce gold-oxidized species, leading to higher conversions and economy of reactants. Our study highlights the intriguing and complex mechanisms of mechanochemical systems, in addition to fostering the atom and energy economy side of mechanochemical means to produce metal nanoparticles.

Received 17th November 2023,
Accepted 21st March 2024

DOI: 10.1039/d3cp05609k

rsc.li/pccp

Introduction

The advances in metal nanoparticles (NPs) synthesis vastly contributed to the expansion of the nanoscience domain, enabling precise tailoring over materials properties *via* manipulation of size, morphology, and composition.[1–3] Such control of NPs features has been achieved by choosing the appropriate stabilizers,[4] reducing agents,[5] solvent, and synthesis temperature in the chemical reduction of metal precursors.[2,6,7] By adjusting these synthesis parameters, one tries to control the balance between the kinetic and thermodynamics of NPs nucleation and growth,[8,9] and, therefore, the final characteristics of the NPs. Most synthesis approaches rely on solution-based protocols, making an outstanding physicochemical control of the final NPs possible.[2] On the other hand, the reactions are generally conducted in thermal or solvent-intensive conditions or both. Additionally, the significant use of surfactant agents to mitigate particle aggregation introduces additional challenges associated with subsequent purification procedures.[4]

Mechanochemical synthesis employing ball milling has been progressively established as a greener and more versatile alternative to conventional solution-based methods.[10,11] Mechanochemical routes offer enhanced reproducibility, superior yields, and eliminate or reduce the need for solvents.[10,11] In recent mechanochemical syntheses of noble metal NPs, such as Ag, Au, and Pd NPs, the procedures involve milling the metal salt precursor and reductants.[12–21] Typical reducing agents such as sodium borohydride, ascorbic acid, sodium citrate, and hydroquinone have commonly been employed in conjunction with stabilizing agents like polyvinylpyrrolidone (PVP), aliphatic amines, or supports such as silica (SiO_2)[12–20] and porous systems.[22,23] In specific cases, bio-sourced molecules have also been reported as reducing and stabilizing agents.[24–27]

[a] *Institute of Chemistry, University of São Paulo – Av. Prof. Lineu Prestes 748, 05508-000, São Paulo – SP, Brazil. E-mail: paulofmo@usp.br*
[b] *Brazilian Synchrotron Light Laboratory (LNLS), Brazilian Center for Research in Energy and Materials (CNPEM), Campinas – SP, 13083-970, Brazil*

† Electronic supplementary information (ESI) available. See DOI: https://doi.org/10.1039/d3cp05609k

This bottom-up approach tends to enable better control over the size and shape of NPs[15] in contrast to the methods of reducing the particle size of bulk metals by milling (top-down)[28] or mechanical decomposition.[29,30]

However, the comprehensive understanding of the underlying mechanisms of NPs formation, especially from a fundamental viewpoint of kinetics and thermodynamics, is very limited. Notably, recent investigations have revealed a disparity between the expected chemical reduction rates observed in solution-based syntheses of AuNPs and those observed in mechanochemical syntheses.[18] The studies showed that ascorbic acid and hydroquinone reductants, priorly considered of mild strength, could reduce Au^{I} salt within minutes. In contrast, while using $NaBH_4$, which is one of the strongest reducing agents, the reaction did not complete after hours of continuous milling.[18] A recent thermodynamic model for the bottom-up mechanochemical synthesis (BUMS) of AuNPs indicated that a ballistic driving force[31] (from the external use of mechanical forces) reduces the activation energy barrier for reaction and affects the nucleation and growth of the nanocrystals.[32] The theorical model agrees well with experimental results of amine stabilized AuNPs.[19] These recent results clearly indicate that only a little knowledge can be borrowed from solution chemistry, reinforcing the need of fundamental investigations of mechanochemical systems.

To continue our recent efforts to understanding the mechanisms of bottom-up mechanochemical synthesis (BUMS) of AuNPs (by the chemical reduction of metal precursors),[18] in the present article we further investigate the use of common reducing agents in their stoichiometric-limited conditions. This means that, while in most of the cases an excess of the reducing agent is necessary to produce metal NPs in reasonable time, we choose to work in the stoichiometry and sub-stoichiometry conditions determined by the redox balanced reactions. The chemical reactions of metal salt precursor, *i.e.*, the very first step for NPs formation, were followed by X-ray absorption near edge spectroscopy (XANES). XANES shows that the use hydroquinone and ascorbic acid even in sub-stoichiometry amounts can induce the complete reduction of the metal salts within minutes of ball-milling. Powder X-ray diffraction (PXRD) was used to evaluate the crystallinity of the NPS, while the analysis of subproducts from the oxidized reducing agents were analyzed by ^{1}H NMR and CG-FID/MS. The dynamic of salt reduction and NP formations is accompanied by the regeneration of hydroquinone from its most oxidized form, *p*-benzoquinone. In addition, other subproducts were generated during the milling process, notably chlorinated aromatics. Our studies on AuNPs demonstrate the potential for optimizing precursor reduction under sub-stoichiometric conditions of the reducing agents. This offers the prospect of developing environmentally friendly and more cost-effective alternatives for metal NPs production.

Experimental methods

Materials

All materials were obtained from commercial suppliers: $HAuCl_4 \cdot 3H_2O$ (99%, Sigma-Aldrich), L-ascorbic acid (AA, 99%, Sigma-Aldrich), hydroquinone (HQ, 99.5%, Sigma-Aldrich), $NaBH_4$ (98%, Sigma-Aldrich), silicon dioxide (SiO_2, 99%, Sigma-Aldrich, 500 $m^2\ g^{-1}$), acetonitrile (ACN, 99.9%, Sigma-Aldrich) and deuterium oxide (D_2O, 99.95%, Sigma-Aldrich).

Bottom-up mechanochemical synthesis of AuNPs

The mechanochemical syntheses were conducted using a Pulverisette 23 vibratory mill (P23, Fritsch®), operating at 50 Hz, with a single zirconia ball ($\varnothing$ = 10 mm, 3 g), and a 10 mL X-ray transparent PMMA jar. The bottom-up mechanochemical syntheses were performed using the salts $HAuCl_4 \cdot 3H_2O$, in the presence of a reducing agent (R_A) and SiO_2 as solid support, considering balanced redox equations (ESI,† Tables S1–S3). Amorphous SiO_2 was washed several times prior to synthesis with solvents of different polarities to remove possible adsorbed species. Amorphous SiO_2 was selected over other oxides because it is highly stable in reducing media, not engaging in the reduction process. Additionally, amorphous SiO_2 displays a high specific surface area at the beginning of the milling period (500 $m^2\ g^{-1}$), which helps prevent nanoparticle aggregation. Additionally, metal NPs supported on SiO_2 have been successfully prepared without the need for surface agents, making the final materials very attractive as catalysts.

The synthesis conditions, including the amounts of the reactants, can be found in the Table 1. For each synthesis, the metal to support agent (SiO_2) ratio was kept approximately constant to eliminate potential interferences from metal distribution. Additionally, an equal total mass was standardized for each synthesis, minimizing errors arising from kinetic effects and energy distribution during impacts (ball-to-powder mass ratio). The metal precursor ($HAuCl_4 \cdot 3H_2O$) is highly hygroscopic and a certain amount of salt can be dissolved by the atmospheric moisture during weighing, reducing its crystallinity. Hence, the metal precursor was carefully weighed onto the silica within the milling jar. In addition, prior to the addition of the reducing agent, the gold salt and SiO_2 underwent a 5-min milling process to pulverize and distribute the salt all over the support.

Analytical methods

Powder X-ray diffraction (PXRD) was used to investigate the crystallinity of the final samples. The size and morphology of the final NPs were determined by transmission electron

Table 1 Composition of reactant mixtures employed in BUMS of Au nanoparticles using $HAuCl_4 \cdot 3H_2O$ as gold source

Reducing agent (R_A)	Salt : R_A stoichiometric	Salt (mg)	R_A (mg)	Salt : R_A experimental
$NaBH_4$	1 : 3/8	27.3	2.1	1 : 3/4[c]
AA	1 : 3/2	14.1	14.5	1 : 3[c]
HQ_{sto}	1 : 3/2	14.5	6.5	1 : 3/2[a]
HQ_{sub}		14.0	3.2	1 : 3/4[b]
HQ_{exc}		14.8	12.6	1 : 3[c]

[a] Stoichiometric amounts of R_A (sto). [b] Sub-stoichiometric amounts of R_A (sub). [c] Twice stoichiometric amounts of R_A – excess (exc). Overall mass including all reactants and SiO_2 = 200 mg.

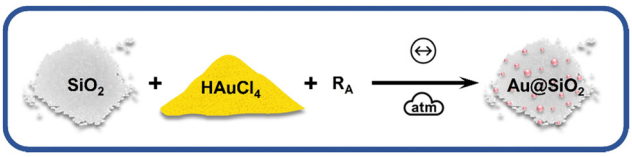

Fig. 1 Scheme of BUMS of AuNPs using SiO_2 solid support and $AuCl_4^-$ as gold source. R_A = HQ, $NaBH_4$ or AA. Symbols used according to ref. 33.

microscopy (TEM). CG-FID, GC-MS and ^1H NMR were used to determine the subproducts of hydroquinone reactions. X-Ray absorption near edge spectroscopy (XANES) was used to follow the chemical reduction of Au salt to Au(0). XANES acquisitions were performed at Tarumã end-station of Carnaúba beamline (Sirius, LNLS/CNPEM). All the details of the analytical methods can be found in the ESI.†

Results and discussion

The reactions under ball milling conditions were conducted using SiO_2 as a solid support for NPs stabilization instead of polyvinylpyrrolidone (PVP) as a capping agent as done previously.[18] Thus, in addition to study the stoichiometric amounts of the reducing agents, we could extend our investigation to the effect of the stabilizing system on the kinetics of the chemical reduction of the metal salts and on the final NPs. The chemical reduction of $HAuCl_4 \cdot 3H_2O$, source of Au^{III}, by the appropriate R_A (Fig. 1) was monitored *ex situ* by XANES at Carnaúba beamline (Sirius, LNLS/CNPEM). X-Ray absorption spectroscopy (in XANES region) was chosen to monitor the oxidation state of Au species in the L_3-edge (11 919 eV). This energy specifically corresponds to the excitation energy of $2p_{3/2}$ electrons to 5d valence states. Thus, the reduction of Au^{III} species to Au(0) is accompanied by an energy shift in the absorption spectrum towards higher energies and a decrease in white line intensity, reflecting a lower density of unoccupied 5d states.

We first investigated the use of twice the stoichiometric amounts necessary to reduce one mol of Au^{III} salt to its metallic form according to the balanced redox reaction (Table S3, ESI†), *i.e.*, the R_A is present in excess. Based on the standard electrochemical cell potentials (ΔE^0_{cell}), the chemical reactions are thermodynamically favored for all reducing agents considered in this study. Fig. 2A–C displays the XANES spectra with R_A = $NaBH_4$, AA and HQ used in one mol excess. The XANES spectra suggest a greater reduction extension from Au^{III} to Au(0) within minutes when AA and HQ were used, while $NaBH_4$ did not lead to good conversion even after 60 min of milling. The kinetics of the chemical reaction for Au(0) formation was followed by the spectral composition, which was obtained from the linear combination fitting (LCF) of the XANES spectra for each milling time (Fig. 2D–F). The LCF indicates that in one min of milling, AA and HQ were able to reduce the Au^{III} in 34% and 88%, respectively. On the other hand, when $NaBH_4$ was used, the reduction reaction barely converted 50% of Au^{III} after 60 min Fig. 2D. This behavior is similar to the previous chemical reduction of Au^I using a PVP in the stabilizing system, where HQ and AA were more efficient in terms of chemical kinetics than $NaBH_4$ for AuNP formation.[18] When this present study is compared to our previous work in terms of the stabilizing system using either a capping agent (PVP) or a support (SiO_2), apparently there is no effect on the nature of the solid matrix. PVP is an organic polymer, where HQ and AA could interact and disperse better enhancing the chemical reduction of Au salt in

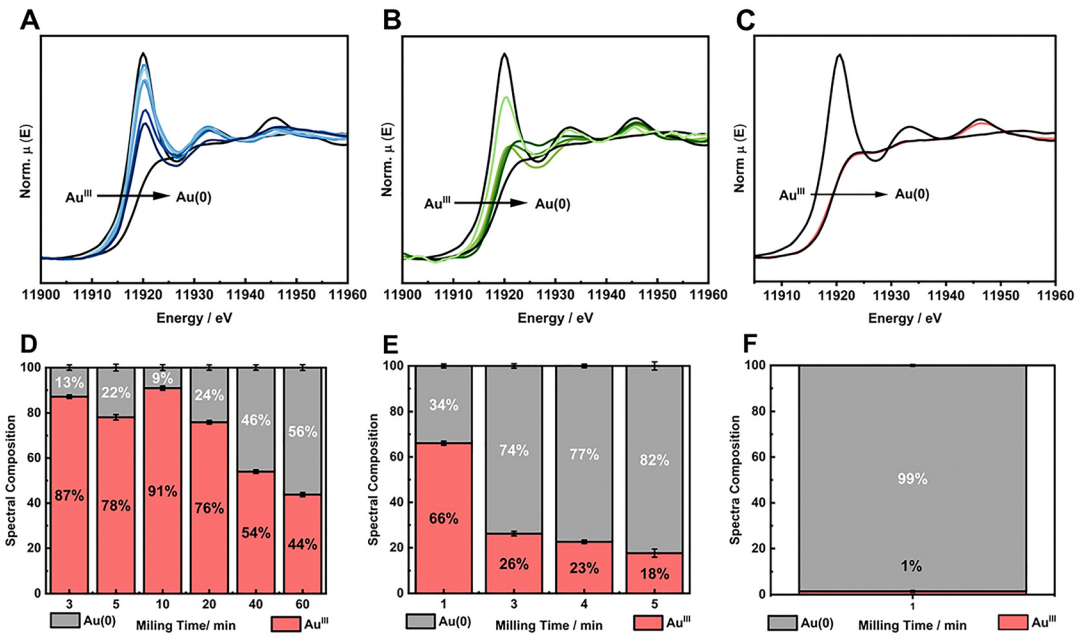

Fig. 2 XANES spectra probing Au–L_{III} edge for BUMS of Au NPs under ball milling conditions using excess of $NaBH_4$ (A), L-ascorbic acid (green spectra, B) and HQ (red spectra, C). The black spectrum in all graphics corresponds to $AuCl_4^-$ and Au NPs standards. (D)–(F) Correspond to the spectral composition obtained by LCF of gold standards and the measured spectra using $NaBH_4$, L-ascorbic acid and HQ as reducing agents, respectively.

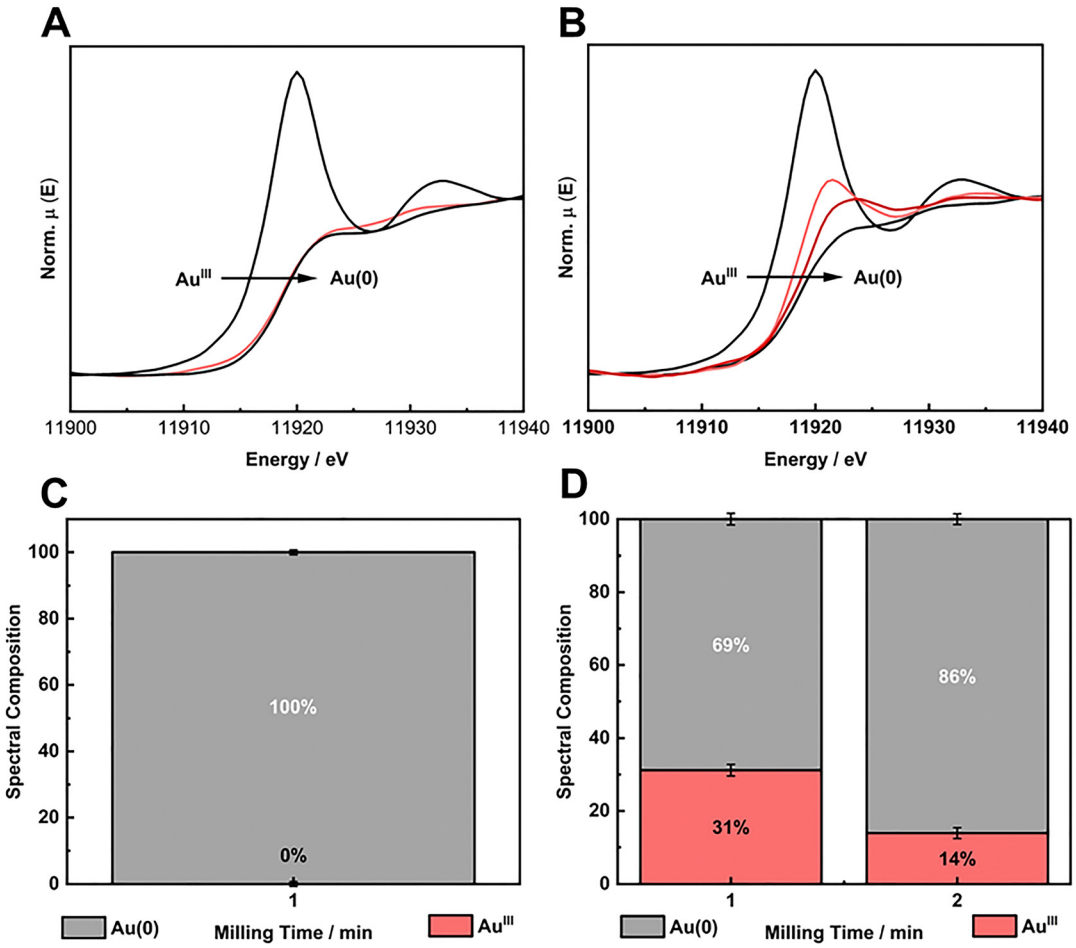

Fig. 3 XANES spectra (Au–L_{III} edge) for the stoichiometric – HQ_{sto} (A) and sub-stoichiometric – HQ_{sub} (B) BUMS of Au NPs using HQ as reducing agent. The black spectrum in the graphics corresponds to $AuCl_4^-$ and Au NPs standards. (C) and (D) Correspond to the spectral composition obtained by LCF of gold standards and the measured spectra of the samples.

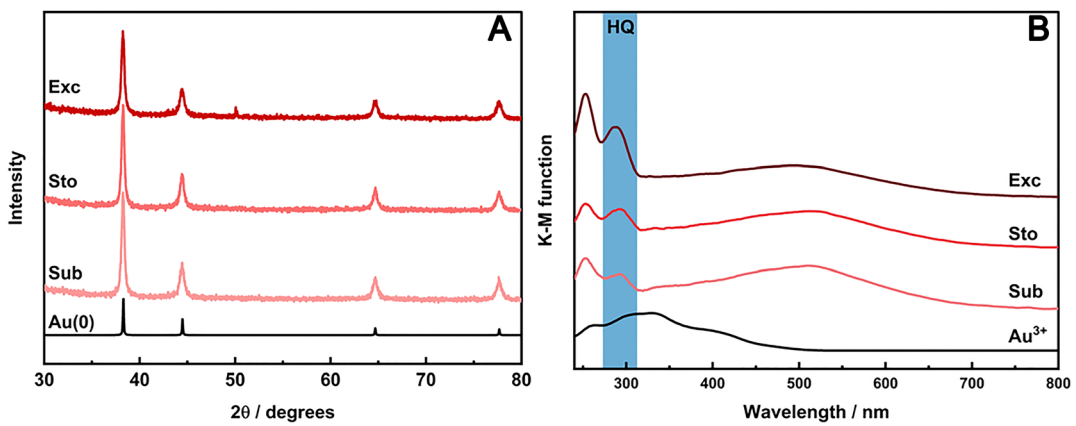

Fig. 4 *Ex situ* PXRD measurements were conducted after ball milling synthesis for $HAuCl_4{\cdot}3H_2O$ reduction by HQ (A), and UV/VIS DRS spectra of the same samples (B) and under stoichiometric, sub-stoichiometric, and excess of R_A.

the whole medium,[34–36] while SiO_2 could, theoretically, disperse better ionic species such as $Na^+BH_4^-$ due to coulombic interactions. The results obtained herein, however, demonstrate that regardless the stabilizing solid, HQ is the most effective reducing agent to transform Au oxidized forms into metallic Au.

The much faster kinetics of the chemical redox reaction when HQ was used as reducing agent required further

Table 2 Hypotheses for complete conversion of Au^{III} using HQ in sub-stoichiometric amounts along with the description of related experiments and the analytical results

Entry	Hypotheses	Experiment	Analytical results
A	Subproducts of HQ oxidation can reduce Au^{III}.	Analysis of HQ subproducts of the reaction Au^{III}:HQ_{sub}	Detection of BQ, HQ and their chlorinated derivatives[a]
B	BQ[d] reduces Au^{III}	Milling Au^{III}, BQ and SiO_2	Formation of Au(0) NPs[b] and detection of BQ, HQ and their chlorinated derivatives[a]
C	BQ is reduced to HQ in the presence of Au(0)	1 – milling BQ with clean/washed AuNPs@SiO_2 2 – milling BQ and SiO_2	1 and 2 – BQ only. Neither HQ nor derivatives were detected[a]
D	Is HCl needed to produce HQ from BQ?	1 – milling BQ with as prepared AuNPs@SiO_2 (presence of HCl) 2 – milling BQ and SiO_2 w/HCl	1 and 2 – detection of BQ, HQ and their chlorinated derivatives[a]
E	HQ is formed from BQ in solution?	Synthesis of HQ in ACN under reflux from BQ in acidic medium during 2 h	BQ only. No HQ or derivative was detected[a]
F	BQ can reduce Au^{III} in solution?	Synthesis of AuNPs from Au^{III} with BQ as R_A in aqueous medium during 2 h at 70 °C	Au^{III} species remained in the media[c]

Determined by: [a] GC-MS, GC-FID and ^{1}H NMR. [b] PXRD. [c] UV/VIS. ACN – acetonitrile. [d] BQ: benzoquinone – product of complete oxidation of HQ.

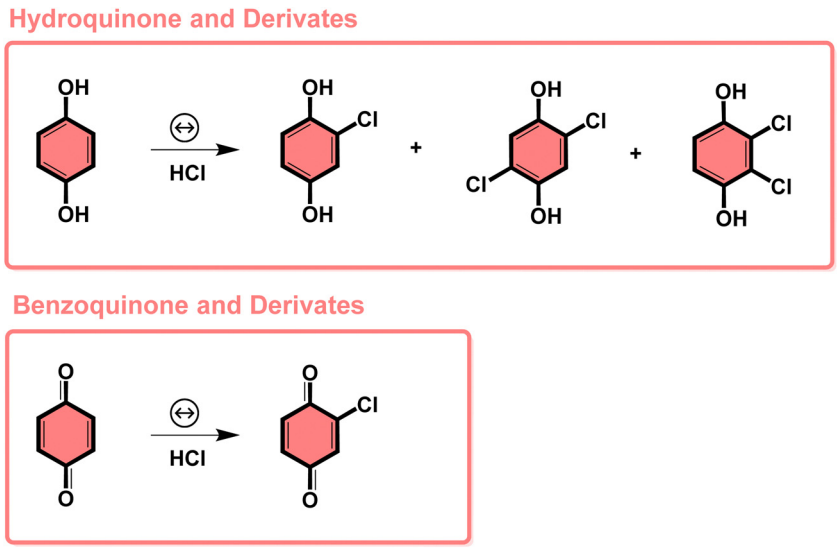

Fig. 5 Subproducts of the BUMS of AuNPs from $AuCl_4^-$ precursor and HQ_{sub} as reducing agent, determined by GC-FID and GC-MS or ^{1}H NMR in solution.

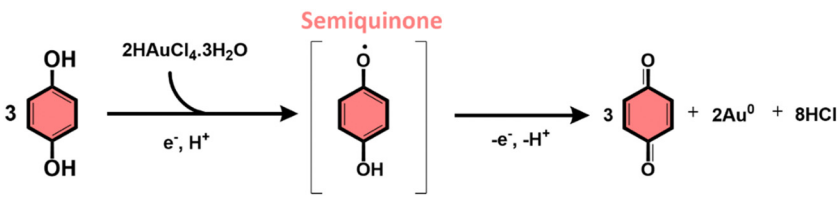

Fig. 6 Mechanism of electron transfer from HQ to reduce Au^{x+} and consequent generation of BQ.

exploration of the effect of its amount in the reaction medium. Thus, we choose to work with limited amounts of HQ for Au^{III} reduction. Two other Au^{III}:HQ ratios were studied: (i) the stoichiometric amount – HQ_{sto} (1 : 3/2) and (ii) the use of sub-stoichiometric quantities of HQ – HQ_{sub} (1 : 3/4). In this last case, we aimed to understand the limitation of HQ load to solely partially reduce the Au salt in BUMS conditions. In other words, HQ is the limiting reactant, and therefore, we would be able to determine the amount of Au salt that could actually be reduced by such amount of HQ. The XANES spectra and the respective LCF for Au^{III} reduction with HQ shows that for stoichiometric and sub-stoichiometric, the reactions proceeded in good to excellent conversion, respectively (Fig. 3A–D).

The crystallinity of AuNPs prepared with HQ in stoichiometric and sub-stoichiometric ratios as well as in molar excess were assessed by PXRD at the end of each milling procedure

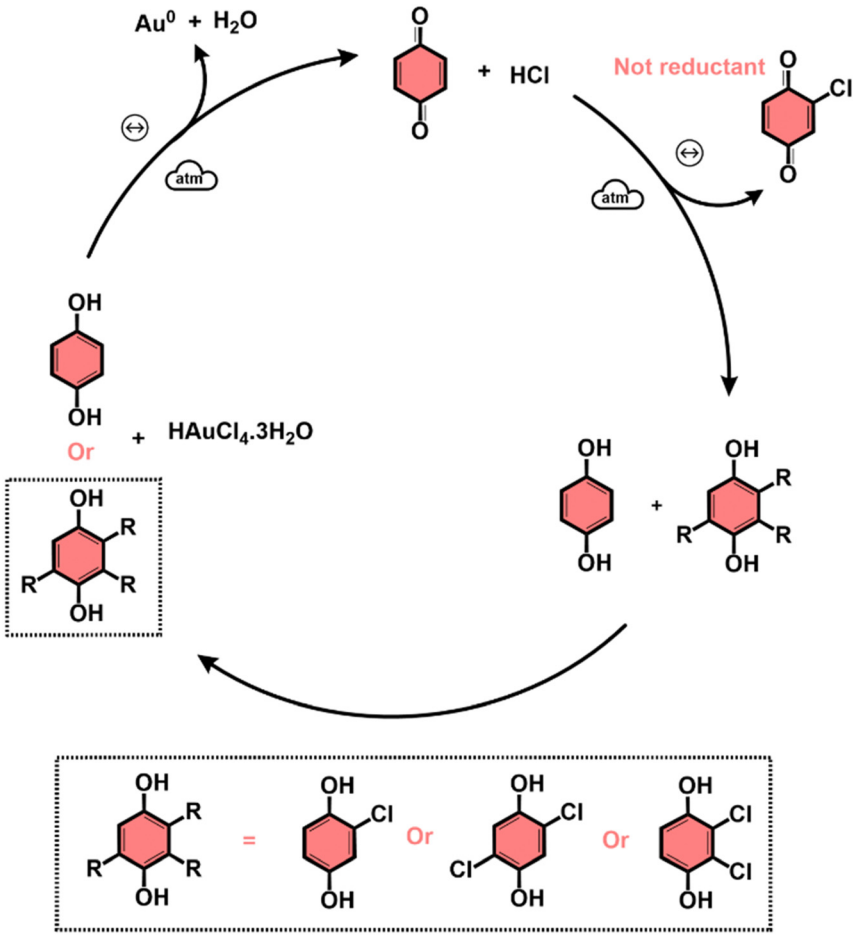

Fig. 7 Proposed mechanism of bottom-up mechanochemical synthesis of AuNPs using HQ in limiting (or sub-stoichiometric) conditions. HQ is regenerated from BQ in acidic media and under mechanochemical conditions, being able to reduce the remaining Au^{III} species.

(Fig. 4A). The PXRD patterns show Bragg reflections at 2θ angles of 38.18°, 44.37°, 64.55°, 77.54°, and 81.69° (using Cu Kα). These reflections respectively correspond to the *d*-spacing of (111), (200), (220), (311) planes, consistent with fcc crystal structure (ICSD 52249) of metallic gold. Notably, no traces of HQ or the respective oxidized products were detectable in the PXRD. The poor intensity and the broadening of the characteristic reflections of metallic gold in the PXRD patterns indicate the nanosized domain of the formed Au crystals. AuNPs were also analyzed by TEM for the synthesis using HQ in different ratios (Fig. S6, ESI†), confirming the nanocrystal domain of the particles. TEM also reveals that as we increase the HQ content, the final particle size is reduced, indicating a faster nucleation for the short milling time used in our experiments.

UV/VIS-DRS also confirmed the nanosize of AuNPs due the presence of the localized surface plasmon resonance (LSPR) band, characteristic of Au nanostructures. A LSPR band is observed in the DRS spectra (Fig. 4B) for samples, irrespective the amount of HQ used. This band in the VIS range peaks around 520 nm and matches the region of the LSPR of roundish Au nanoparticles. Interestingly, a band in the UV region around 287 nm could also be observed in the spectra for all three Au^{III}:HQ ratios used in the mechanochemical reactions, increasing accordingly to the amounts of HQ in the media. This band would be related to the residual traces of the HQ. However, at least in the sub-stoichiometric reaction, the complete consumption of the reducing agent (R_A) should be expected, and, therefore, no remaining HQ should be detected in the UV/VIS spectra.

In the mechanochemical synthesis of AuNPs using sub-amounts of HQ, there are two intriguing controversies revealed by XANES (Fig. 3B and D) and UV/VIS DRS (Fig. 4B): first, how the use of a sub-stoichiometric quantity of a reducing agent can lead the reaction to conversion higher than the 50% expected, and, second, how it is still possible to have remaining HQ detected in the UV/VIS at the end of the reaction if this R_A is the limiting reactant. This unusual behavior of HQ in the reaction was further investigated by XANES and conventional analytical techniques such as CG-FID, CG-MS and ^{1}H NMR.

Firstly, we milled Au^{III} salt with SiO_2 only, *i.e.*, without HQ, to check if there would be any reduction due to possible SiO_2 surface groups. The XANES spectrum (Fig. S2, ESI†) shows that after one hour of continuous milling with the same milling parameters, the Au species remained highly oxidized as Au^{III}. Thus, according to XANES, no chemical reduction occurs in

absence of HQ. Therefore, any additional contribution to the reduction reaction due to the solid support alone can be excluded. We then investigated the products of the oxidation of HQ. We aimed to identify the subproducts generated at the end of the redox reaction to investigate the possibility of these chemical species formed of being additional reductants. Table 2 summarizes the experiments adopted to explore the subproduct formation. The experiments displayed on Table 2 were designed to give some insights concerning a mechanism enabling a larger reaction extent despite using HQ in lower amounts than the theoretically required for complete conversion of Au^{III}. Table 2 also contains the hypotheses tested and the respective analytical results.

The subproducts generated during the mechanochemical synthesis of AuNPs using HQ_{sub} (after 2 min milling) were extracted in acetonitrile and analyzed by CG-MS (or CG-FID) and ^1H NMR (Table 2, entry A). As expected, the results revealed the benzoquinone (BQ) is one of the subproducts. BQ is the product of the complete oxidation of HQ (Fig. 6). In addition to BQ, a diversity of chlorinated HQ and BQ derivatives, apart from some HQ were also found in the medium after milling (Fig. 5). Chlorinated derivatives are certainly formed due to the reaction between HQ or BQ with HCl formed in the media upon Au^{III} reduction. Au^{III} (actually $HAuCl_4{\cdot}3H_2O$) is a strong acid. The release of HCl in a medium containing HQ and BQ could lead to the formation of such chlorinated species.

From the products identified by CG-MS, obviously HQ itself, but other chlorinated-HQ derivatives are chemical species that can serve as reducing agents for Au^{III}. This is because the electron transfer reactions are still thermodynamically favored. In fact, the chlorinated-HQs were usual chemical reactants as developing agents for Ag reduction for contrast in photography.[37] The typical mechanism for HQ oxidation is highlighted in Fig. 6.

On the other hand, the reduction of Au salt by BQ is unfavored, because the molecule is already the most oxidized form of HQ, lacking reasonable electrons for further oxidation processes. The same probably applies to any BQ derivative. As show in the mechanism of HQ oxidation, up two electrons can be transferred from each >C–O–H bond of HQ molecule, which is not possible when the molecule is in the BQ configuration (>C=O). However, an experiment starting from Au^{III} and BQ shows that metallic AuNPs also are formed (Table 2, entry B) along with HQ in considerable amounts and other derivatives (see Fig. S4 for PXRD, ESI†). The only plausible explanation for the presence of HQ in medium initially containing only BQ is the chemical reduction of the latter.

Entry C in Table 2 displays the experiments used to study the effect of AuNPs in the mechanism of production of HQ from BQ. The results demonstrated HQ is not formed by milling BQ without AuNPs, and even when the NPs are present in the medium, only traces of HQ is detected. These two experiments, using SiO_2 only and clean AuNPs@SiO_2, share a factor, which is the absence of HCl in medium. Additional experiments then proved that HCl in the media is mandatory for the formation of HQ (Table 2, entry D). In this same set of milling reactions, we noticed that AuNPs are not necessary to induce the reduction of BQ into HQ, because milling BQ with SiO_2 and traces of HCl, HQ can also be formed (Table 2, entry D). Finally, we could demonstrate that HQ and its derivatives, as well as BQ derivatives, can only be formed under mechanochemical conditions. In the conditions we used in solution for HQ formation from BQ in acidic medium (Table 2, entry E), no HQ was detected by GC-FID, and only BQ remained after 2 h in ACN under reflux. This result immediately indicates that if no chemical species capable of reducing Au^{III} to Au(0) are formed, it is not possible to produce AuNPs with BQ as start reactant in solution. This hypothesis was confirmed by a test reaction using BQ, and Au^{III} precursor, where at the end of 2 h at 70 °C in aqueous media, no NP was observed (Table 2, entry F).

Based on our results, we proposed a general qualitative mechanism for BUMS of AuNPs using HQ in sub-stoichiometric conditions (Fig. 7). The scheme in Fig. 7 shows that the successful additional reduction of Au^{III} into metallic Au is possible due to the *in situ* regeneration of HQ and formation of its derivatives, which can reduce the remaining $AuCl_4^-$. The reduction of Au^{III} by the additional of HQ at the beginning of the milling procedure is then followed by the continuous release of HCl in the media and formation of BQ. Then, as the milling continues, BQ, HCl and some water in the media (from $HAuCl_4{\cdot}3H_2O$), HQ is regenerated, which in turn, can reduced remaining Au^{III}. Also, chlorinated HQ derivatives are formed, which can also act as reductants. Chlorinated BQ-derivatives are also formed under mechanochemical conditions as byproducts.

Conclusion

The bottom-up mechanochemical synthesis of AuNPs from the chemical reduction of $AuCl_4^-$ over amorphous SiO_2 was investigated. *Ex situ* XANES at Au–L_3 edge and subsequently linear combination fitting were used to monitor the chemical reaction by following the reduction of Au^{III}. $NaBH_4$, L-ascorbic acid (AA), and hydroquinone (HQ) were used as reducing agents in excess (exc). AA_{exc} and HQ_{exc} could reduce a much larger amount of Au^{III} in few minutes (<5 min) under milling conditions, while the reaction with $NaBH_4$ reached only 56% of conversion after 60 min of milling. The LCF of XANES spectra also showed the superior performance of HQ_{exc} as reducing agent in terms of chemical reaction rate.

Extending the studies to the use of stoichiometric-limited amounts of HQ, either in stoichiometric (HQ_{sto}) and sub-stoichiometric (HQ_{sub}) conditions, we observed that it was still possible to reduce Au^{III} to a greater extent than theoretically possible, especially for the case of HQ_{sub}. UV/VIS DRS evidenced the intriguing presence of HQ in the medium after the reaction. After a series of probing experiments and GC-MS, GC-FID and ^1H NMR analyses of the organic byproducts originated from the initial HQ, we could demonstrate that HQ itself can be regenerated from its oxidized counterpart, benzoquinone (BQ). Nonetheless, the HQ formation from BQ

was only observed under mechanochemical and acidic conditions. The source of electrons for BQ reduction, however, is not yet known and further studies should address this specific issue. During the milling procedure, chlorinated derivatives were also detected as byproducts, from the reaction of the aromatic compounds with chloride of the Au salt. The regenerate HQ and its chlorinated derivatives can conclude the reduction of the remaining $AuCl_4^-$ when HQ is used in sub-stoichiometric amounts. TEM images showed the amount of HQ affect the size of NPs, by acting in the nucleation step. As expected, the higher the amount of HQ the smaller the size of the NPs.

The results presented herein demonstrate the complexity of events and a variety of reactions induced by mechanical milling of a somehow considered typical reduction–oxidation chemical reaction. Apart from the advances in the understanding mechanochemical reactions and BUMS of NPs, our results also represent a step towards designing efficient and cost-effective metal nanoparticle syntheses, using less quantities of chemicals in a reduced reaction time. Finally, the unexpected behavior of the reactional medium reveals a route for halogenation of aromatics from hydrochloric acid.

Author contributions

I. P. L. X.: data curation, formal analysis, investigation, writing – original drafts; L. L. L.: investigation, formal analysis; E. C. M.: investigation; E. T. C.: investigation; B. L. S.: investigation, data curation; L. A. F.: investigation, data curation; D. G.: methodology; P. F. M. O.: conceptualization, data curation, supervision, methodology, writing – review & editing.

Conflicts of interest

The authors declare no competing financial interest.

Acknowledgements

This research used facilities of the Brazilian Synchrotron Light Laboratory (LNLS), part of the Brazilian Center for Research in Energy and Materials (CNPEM), a private, non-profit organization under the supervision of the Brazilian Ministry for Science, Technology, and Innovation (MCTI). The CARNAUBA beamline staff is acknowledged for their assistance during the experiments 20220095. The following authors thank Sao Paulo Research Foundation (FAPESP) for funding – (Author, Fellowship number) – IPLX, 2023/01223-5; LLL, 2022/03996-9; BLS, 2019/09341-1; LAF, 2022/04604-7. ECM and ETC thank CAPES (88882.328255/2019-01) and CNPq (131191/2021-7), respectively. PFMO acknowledge FAPESP (Grant 2020/14955-6).

References

1 W. Niu and X. Lu, in *Metallic Nanostructures*, ed. Y. Xiong and X. Lu, Springer International Publishing, Cham, 2015, pp. 1–47.
2 Y. Xia, Y. Xiong, B. Lim and S. E. Skrabalak, Shape-Controlled Synthesis of Metal Nanocrystals: Simple Chemistry Meets Complex Physics?, *Angew. Chem., Int. Ed.*, 2009, **48**, 60–103.
3 Y. Shi, Z. Lyu, M. Zhao, R. Chen, Q. N. Nguyen and Y. Xia, *Chem. Rev.*, 2021, **121**, 649–735.
4 T. H. Yang, Y. Shi, A. Janssen and Y. Xia, *Angew. Chem., Int. Ed.*, 2020, **59**, 15378–15401.
5 T. S. Rodrigues, M. Zhao, T. Yang, K. D. Gilroy, A. G. M. da Silva, P. H. C. Camargo and Y. Xia, Synthesis of Colloidal Metal Nanocrystals: A Comprehensive Review on the Reductants, *Chem. – Eur. J.*, 2018, **24**, 16944–16963.
6 F. Fiévet, S. Ammar-Merah, R. Brayner, F. Chau, M. Giraud, F. Mammeri, J. Peron, J.-Y. Piquemal, L. Sicard and G. Viau, The polyol process: a unique method for easy access to metal nanoparticles with tailored sizes, shapes and compositions, *Chem. Soc. Rev.*, 2018, **47**, 5187–5233.
7 W. Li, M. G. Taylor, D. Bayerl, S. Mozaffari, M. Dixit, S. Ivanov, S. Seifert, B. Lee, N. Shanaiah, Y. Lu, L. Kovarik, G. Mpourmpakis and A. M. Karim, Solvent manipulation of the pre-reduction metal–ligand complex and particle-ligand binding for controlled synthesis of Pd nanoparticles, *Nanoscale*, 2021, **13**, 206–217.
8 Y. Xia, X. Xia and H.-C. Peng, Shape-Controlled Synthesis of Colloidal Metal Nanocrystals: Thermodynamic versus Kinetic Products, *J. Am. Chem. Soc.*, 2015, **137**, 7947–7966.
9 Y. Wang, J. He, C. Liu, W. H. Chong and H. Chen, Thermodynamics versus Kinetics in Nanosynthesis, *Angew. Chem., Int. Ed.*, 2015, **54**, 2022–2051.
10 W. Jones and M. D. Eddleston, Introductory Lecture: Mechanochemistry, a versatile synthesis strategy for new materials, *Faraday Discuss.*, 2014, **170**, 9–34.
11 T. Friščić, C. Mottillo and H. M. Titi, Mechanochemistry for Synthesis, *Angew. Chem., Int. Ed.*, 2020, **59**, 1018–1029.
12 D. Debnath, S. H. Kim and K. E. Geckeler, The first solid-phase route to fabricate and size-tune gold nanoparticles at room temperature, *J. Mater. Chem.*, 2009, **19**, 8810–8816.
13 D. Debnath, C. Kim, S. H. Kim and K. E. Geckeier, Solid-state synthesis of silver nanoparticles at room temperature: Poly (viny lpyrrolidone) as a toola, *Macromol. Rapid Commun.*, 2010, **31**, 549–553.
14 P. F. M. de Oliveira, J. Quiroz, D. C. de Oliveira and P. H. C. Camargo, A mechano-colloidal approach for the controlled synthesis of metal nanoparticles, *Chem. Commun.*, 2019, **55**, 14267–14270.
15 P. F. M. de Oliveira, R. M. Torresi, F. Emmerling and P. H. C. Camargo, Challenges and opportunities in the bottom-up mechanochemical synthesis of noble metal nanoparticles, *J. Mater. Chem. A*, 2020, **8**, 16114–16141.
16 R. T. P. da Silva, S. I. Córdoba De Torresi and P. F. M. de Oliveira, Mechanochemical Strategies for the Preparation of SiO_2-Supported AgAu Nanoalloy Catalysts, *Front. Chem.*, 2022, **10**, 1–10.
17 P. F. M. de Oliveira, A. A. L. Michalchuk, A. G. Buzanich, R. Bienert, R. M. Torresi, P. H. C. Camargo and F. Emmerling, Tandem X-ray absorption spectroscopy and

scattering forin situtime-resolved monitoring of gold nanoparticle mechanosynthesis, *Chem. Commun.*, 2020, **56**, 10329–10332.
18 P. F. M. de Oliveira, A. A. L. Michalchuk, J. Marquardt, T. Feiler, C. Prinz, R. M. Torresi, P. H. C. Camargo and F. Emmerling, Investigating the role of reducing agents on mechanosynthesis of Au nanoparticles, *CrystEngComm*, 2020, **22**, 6261–6267.
19 M. J. Rak, N. K. Saadé, T. Friščić and A. Moores, Mechanosynthesis of ultra-small monodisperse amine-stabilized gold nanoparticles with controllable size, *Green Chem.*, 2014, **16**, 86–89.
20 T. Premkumar and K. E. Geckeler, Palladium nanostructures: Solvent-less, one-pot mechano-chemical synthesis using poly(vinylpyrolidone) and catalytic activity, *Colloids Surf., A*, 2014, **456**, 49–54.
21 R. A. Haley, J. Mack and H. Guan, 2-in-1: Catalyst and reaction medium, *Inorg. Chem. Front.*, 2017, **4**, 52–55.
22 L. Niu, X. Zhao, Z. Tang, F. Wu, Q. Lei, J. Wang, X. Wang, W. Liang and X. Wang, Solid-solid synthesis of covalent organic framework as a support for growth of controllable ultrafine Au nanoparticles, *Sci. Total Environ.*, 2022, **835**, 155423.
23 X. Li, Z. Zhang, W. Xiao, S. Deng, C. Chen and N. Zhang, Mechanochemistry-assisted encapsulation of metal nanoparticles in MOF matrices via a sacrificial strategy, *J. Mater. Chem. A*, 2019, **7**, 14504–14509.
24 M. Baláž, N. Daneu, Ľ. Balážová, E. Dutková, Ľ. Tkáčiková, J. Briančin, M. Vargová, M. Balážová, A. Zorkovská and P. Baláž, Bio-mechanochemical synthesis of silver nanoparticles with antibacterial activity, *Adv. Powder Technol.*, 2017, **28**, 3307–3312.
25 M. Baláž, Z. Bedlovičová, N. Daneu, P. Siksa, L. Sokoli, L. Tkáčiková, A. Salayová, R. Džunda, M. Kováčová, R. Bureš and Z. L. Bujňáková, Mechanochemistry as an alternative method of green synthesis of silver nanoparticles with antibacterial activity: A comparative study, *Nanomaterials*, 2021, **11**(5), 1139.
26 M. J. Rak, T. Friščić and A. Moores, One-step, solvent-free mechanosynthesis of silver nanoparticle-infused lignin composites for use as highly active multidrug resistant antibacterial filters, *RSC Adv.*, 2016, **6**, 58365–58370.
27 M. J. Rak, T. Friščić and A. Moores, Mechanochemical synthesis of Au, Pd, Ru and Re nanoparticles with lignin as a bio-based reducing agent and stabilizing matrix, *Faraday Discuss.*, 2014, **170**, 155–167.
28 H. Schreyer, R. Eckert, S. Immohr, J. de Bellis, M. Felderhoff and F. Schüth, Milling Down to Nanometers: A General Process for the Direct Dry Synthesis of Supported Metal Catalysts, *Angew. Chem., Int. Ed.*, 2019, **58**, 11262–11265.
29 F. Delogu, Mechanochemical decomposition of Ag and Ni oxalates, *Mater. Chem. Phys.*, 2014, **147**, 629–635.
30 F. Delogu, Ag Nanoparticles from the Mechanochemical Decomposition of Ag Oxalate, *Langmuir*, 2012, **28**, 10898–10904.
31 G. Martin and P. Bellon, *Solid State Phys.*, 1996, **50**, 189–331.
32 L. Yang, A. Moores, T. Friščić and N. Provatas, Thermodynamics Model for Mechanochemical Synthesis of Gold Nanoparticles: Implications for Solvent-Free Nanoparticle Production, *ACS Appl. Nano Mater.*, 2021, **4**, 1886–1897.
33 A. A. L. Michalchuk, E. V. Boldyreva, A. M. Belenguer, F. Emmerling and V. V. Boldyrev, Tribochemistry, Mechanical Alloying, Mechanochemistry: What is in a Name?, *Front. Chem.*, 2021, **9**, 1–29.
34 J. O. Sanchez, Y. Ismail, B. Christina and L. J. Mauer, Degradation of L-Ascorbic Acid in the Amorphous Solid State, *J. Food Sci.*, 2018, **83**, 670–681.
35 S. Ghanbarzadeh, R. Hariri, M. Kouhsoltani, J. Shokri, Y. Javadzadeh and H. Hamishehkar, Enhanced stability and dermal delivery of hydroquinone using solid lipid nanoparticles, *Colloids Surf., B*, 2015, **136**, 1004–1010.
36 P. Bandyopadhyay and F. Rodriguez, Interaction of poly(vinyl pyrrolidone) with phenolic cosolutes, *Polymer*, 1972, **13**, 119–123.
37 H. I. Bjelkhagen, in *Silver-Halide Recording Materials*, ed. A. L. Schawlow, A. E. Siegman and T. Tamir, Springer, Heidelberg, 2nd edn, 1993, ch. 4, pp. 115–158.

